



Imidazo[4,5-b]phenazines as Dual Topoisomerase I/II α Inhibitors: Design, Synthesis, Biological Evaluation and Molecular Docking

Iman A. Y. Ghannam ^{1*}, Ahmed M. El Kerdawy ² and Heba T. Abdel-Mohsen ^{1*}



CrossMark

¹ Department of Chemistry of Natural and Microbial Products, Pharmaceutical and Drug Industries Research Institute, National Research Centre, Dokki, Cairo, 12622, Egypt.

² Department of Pharmaceutical Chemistry, Faculty of Pharmacy, Cairo University, Kasr El-Aini Street, Cairo, P.O. Box 11562, Egypt.

Abstract

In the present study, 1-(un)substituted 2-(hetero)aryl imidazo[4,5-b]phenazines 4a-j and 6a-d were synthesized and evaluated for their cytotoxic activities against a panel of cell lines at 10 micromolar concentration. Compound 4f revealed a remarkable and broad spectrum of cytotoxic activity with growth inhibition percent (GI%) of 11-82%. It was found that cell lines derived from leukemia, and breast cancer were the most sensitive to the imidazophenazine derivative 4f. It showed GI% of 82% against MOLT-4 cell line from leukemia. Moreover, compound 4e showed GI% of 88% against SK-OV-3 cells from ovarian cancer. In addition, compound 4b showed GI% of 51% against M14 melanoma cell line, whereas compound 6a showed GI% of 44% against T-47D breast cancer cell line. The most promising compounds 4a and 4e-g were further tested for their Topo I and Topo II α inhibitory activities. It was found that compound 4e is the most potent derivative against Topo I in comparison to camptothecin (IC₅₀ = 29.25 and 25.71 μ M, respectively), whereas the imidazophenazine derivatives 4f and 4g displayed comparable potency to etoposide against Topo II α (IC₅₀ = 26.74, 22.72, and 20.52 μ M, respectively). Investigation of the effect of compound 4f on MCF-7 cell cycle at its IC₅₀ concentration showed its effectiveness in arresting the cell cycle at the G2/M phase; furthermore, it induced apoptosis in MCF-7 cells. Molecular docking simulations in Topo I and Topo II α revealed that the biological activity of the target compounds could be due to their mechanism of action that resembles the topoisomerase poisons which involves the accommodation of their polycyclic scaffold in the DNA cleavage site stacking between the base pairs interacting through several π - π stacking interactions with the surrounding DNA bases stabilizing the topoisomerase/DNA cleavage complex preventing the re-ligation reaction. Swiss ADME web tool proved that compounds 4f and 4g exhibit promising ADME profile, and drug likeness properties.

Keywords: Imidazophenazines - Topo I/II α inhibitors - Anticancer agents.

1. Introduction

In the recent years, cancer is considered one of the main causes of death worldwide [1, 2]. Most of the clinically used anticancer agents suffer from the lack of selectivity that results in their unfavorable drawbacks [3]. Moreover, the expeditious development of resistance by cancer cells is another challenge that faces most of the currently available anticancer drugs which results in ineffective treatment of malignant tumors [4]. For these reasons,

the development of new, potent, selective, and less toxic anticancer alternatives is an imperative demand in order to cope with these challenges.

In this respect, human topoisomerases are highly overexpressed proteins in several cancer cell-lines to various extents. Hence, DNA topoisomerases were considered one of the main target classes in anticancer drug discovery [5, 6]. Furthermore, in the clinically used cancer treatment regimes, large percentage of the prescribed medications depends on

*Corresponding author e-mail: iman.youssef.ghannam@gmail.com, ia.ghannam@nrc.sci.eg (Iman A. Y. Ghannam); ht.abdel-mohsen@nrc.sci.eg, hebabdelmohsen@gmail.com (Heba T. Abdel-Mohsen)

Receive Date: 28 September 2022, Revise Date: 07 October 2022, Accept Date: 09 October 2022,

First Publish Date: 09 October 2022

DOI: 10.21608/EJCHEM.2022.165869.7040

©2022 National Information and Documentation Center (NIDOC)

using chemotherapeutic agents that efficiently target topoisomerases [7].

DNA Topoisomerases (Topo) are a set of nuclear enzymes that modulate the topology of DNA during replication, transcription and chromatin remodeling [8]. There are two main types of human topoisomerases; topoisomerase type I (Topo I), and type II (Topo II) depending on whether they cleave single or double strands of DNA, respectively [9]. Human Topo II is further sub-classified into topo II α and topo II β . Topo II α is highly overexpressed in proliferating cells enhancing tumor cell growth and division [9]. The cellular Topo II α expression level is highly dependent on the cell cycle. It has its lowest expression level in the G0/G1 phase, then it gradually elevates in the S phase reaching its maximum in the G2/M phase, and finally its level decreases at the end of mitosis phase. On the contrary, Topo II β is not essential for cell survival, and proliferation and its curial role is in cell development, transcriptional regulation, and differentiation. Topo II β is expressed in low level through the different phases of cell cycle. Therefore, topo II α action inhibition is an interesting strategy in cancer therapy by either inducing double-stranded DNA breaks through stabilization of the Topo/DNA cleavage complex or by blocking ATP hydrolysis required for topo machinery energization [10-12].

According to their mechanism of action, topoisomerase inhibitors are classified into two categories [13]; 1) Topo poisons, the major category, which bind to the Topo/DNA cleavable complexes resulting in their stability blocking a key step in the catalytic cycle [14], 2) Catalytic inhibitors which directly inhibit the topoisomerase catalytic activity without DNA breakage [15].

Currently, several important topoisomerase poisons are clinically used for cancer treatment. Camptothecin (I) and its analogues, reversibly block Topo I-mediated cleavage of DNA complex leading to DNA strand breaking which subsequently induces cell apoptosis [16, 17], Meanwhile, Topo II poisons including doxorubicin (II), etoposide (III), and mitoxantrone (IV) inhibit the changes in the topological state of DNA involving the transient double-strand breakage and rejoining of phosphodiester bonds (Fig. 1) [10, 18]. They successfully halt and stabilize the Topo/DNA cleavage complex preventing the re-ligation reaction. This stabilization of the short-lived cleavage complex leads to its trapping and accumulation causing massive genome fragmentation followed by cell death [11, 12].

In the recent years, the combination of topo I and topo II inhibitors demonstrated a superior success in comparison to individual application of topo I or topo II inhibitors. However, this approach failed in the clinical trials due to toxicity issues. Thus, the

utilization of single drug that can target both topo I and topo II simultaneously was proposed [19]. The application of this approach in different tumor models revealed an improved *in vitro* activity with less toxicity in comparison to targeting two individual isoforms [20].

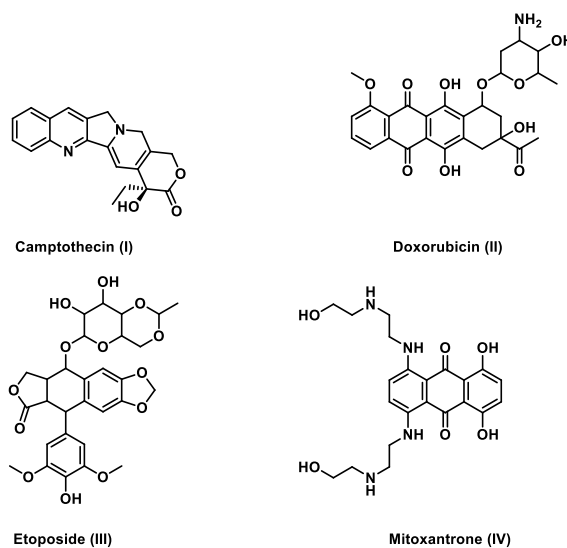


Fig. 1: Structures of topoisomerase I-IV poisons

Molecular hybridization with the aim to develop biologically active molecules is regarded as an interesting strategy for the discovery of novel pharmaceutical active agents [21]. Over the years a wide range of hybrid molecules were synthesized which exhibited improved biological efficacy than their parent molecules. In cancer chemotherapy, it was recognized that combining two pharmacophores with distinct antitumor activity might improve the potency and decrease the adverse effect of the resultant hybrid derivatives [22].

In this regard, phenazine is a well-known polycyclic privileged scaffold whose derivatives are either isolated from natural origins or made available by diverse synthetic methods [23, 24]. Many phenazine derivatives were reported to have promising anticancer activity [24, 25], for instance XR11576 (V) and XR5944 (VI) showed significant *in vitro* and *in vivo* cytotoxic activity [26-28]. Furthermore, XR11576 (V) revealed potent and dual Topo I and Topo II inhibitory activity [29]. Moreover, the antitumor agent NC-190 (VII) demonstrated potent topo II as well as weak topo I inhibitory activity [30].

Recently, Yao *et al.*, displayed the potent cytotoxic activity beside the dual topoisomerase inhibitory activity of a series of 7-alkylamino substituted benzo[*a*]phenazine derivatives. Compound VIII is an example of this series which acted as catalytic inhibitor of Topo II and as a poison of Topo I [31] (Fig. 2).

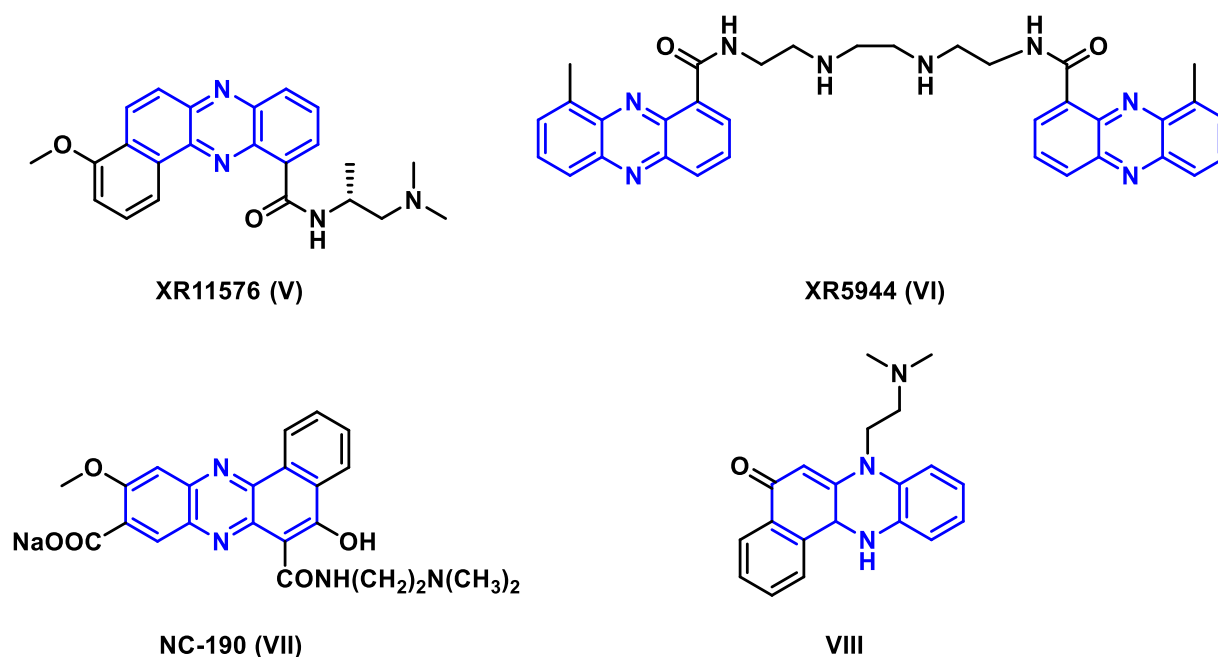


Fig. 2: Structures of phenazines as topoisomerase inhibitors V-VIII

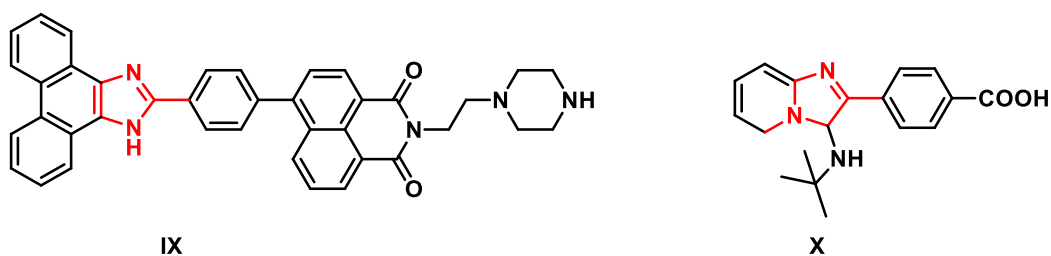
Structures of imidazoles IX and X as topoisomerase II α inhibitors

Fig. 3:

On the other hand, imidazole and fused imidazole are key scaffolds that exist in numerous pharmaceuticals and natural products [32-35]. Imidazoles were linked to diverse polycyclic scaffolds for the synthesis of anticancer agents and topoisomerase inhibitors. For example, Singh *et al.*, [36] reported the synthesis of a new series of naphthalimide-phenanthro[9,10-*d*]imidazole as topoisomerase inhibitors. Compound IX is an example of the presented series displaying potent topoisomerase II α inhibitory activity as well as potent anticancer activity. Moreover, Baviskar *et al.*, [37] reported the discovery of *N*-Fused imidazoles, e.g., compound X, as catalytic topo II α inhibitors (Fig. 3).

Against this background, the molecular hybridization strategy between phenazine (XI) and imidazole XII scaffolds was applied for the design and synthesis of new 1-(un)substituted imidazo[4,5-*b*]phenazines 4a-j and 6a-d as topoisomerase inhibitors and anticancer agents (Fig. 4). The synthesized compounds were subsequently submitted for anticancer screening at NCI-USA at 10 μ M. The most potent hybrid was assayed for its cytotoxic

activity on MCF-7 cell line using SRB assay. Furthermore, it was further investigated for its effect on MCF-7 cell cycle and apoptosis. The ADME properties of the most potent candidates were explored and their molecular docking on topoisomerase I and II α binding sites were investigated.

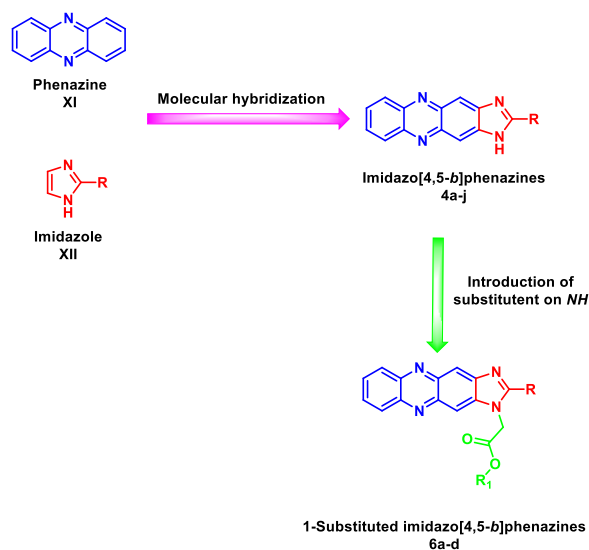


Fig. 4: General rational for the synthesis of the target compounds 4a-j and 6a-d

2. Materials and methods

2.1. Chemistry

Chemicals were supplied from commercial companies. Analytical thin layer chromatography (TLC) was utilized to follow up the progress of the reaction. Elemental analyses and spectral data were carried out at the Micro analytical labs, National Research Centre. Jasco FT/IR 300E Fourier transform infrared spectrophotometer was used to measure IR spectra (4000–400 cm^{-1}). Bruker instruments 300 (75) or 400 (100) MHz were used to measure ^1H NMR and ^{13}C NMR spectra.

2.1.1. Synthesis of phenazine-2,3-diamine (2)

A solution of ceric ammonium nitrate (CAN) (0.1 mmol) in water (10 mL) was added dropwise to a solution of *o*-phenylenediamine (**1**) (1 mmol) in acetone (0.5 mL) with continuous stirring. The reaction mixture was stirred at rt for 96 h then diluted with water and neutralized with NaHCO_3 . The reddish brown precipitate was filtered and dried to give the crude product **2** which was further purified by crystallization from ethanol to give the pure product **2** as a reddish brown powder; mp > 300 °C (Lit. [38] mp > 360 °C).

2.1.2. General Procedure I for the synthesis of 2-substituted imidazo[4,5-*b*]phenazines 4a-j

A mixture of **2** (10 mmol), the aldehyde **3** (10 mmol), acetic acid (0.5 mL) in DMF (25 mL) was stirred under reflux for 4 h. This is followed by down cooling and pouring on ice-water. The precipitated product was filtered with suction and the filter cake was purified by flash chromatography (Pet. Ether / EtOAc 1:1.5 to EtOAc / MeOH 1: 0.05).

2.1.2.1. 2-*p*-Tolyl-1*H*-imidazo[4,5-*b*]phenazine (4a)

Workup gave **4a** as a brown powder; yield = 77 %, mp > 300 °C; ^1H NMR (400 MHz; $\text{DMSO-}d_6$) δ_{H} 2.44 (3H, s), 7.46 (2H, d, $^3J = 8.0$ Hz), 7.86–7.88 (2H, m), 7.92 (2H, d, $^3J = 8.0$ Hz), 8.19–8.23 (2H, m), 8.38 (1H, s) and 8.48 (1H, s) ppm; Anal. Calcd for $\text{C}_{20}\text{H}_{14}\text{N}_4$: C, 77.40; H, 4.55; N, 18.05. Found: C, 77.49; H, 4.64; N, 18.12.

2.1.2.2. 2-(4-Fluorophenyl)-1*H*-imidazo[4,5-*b*]phenazine (4b)

Workup gave **4b** (CAS No. 114991-81-0) as a brown powder; yield = 78 %; mp > 300 °C; $\tilde{\nu}_{\text{max}}$ (atr)/ cm^{-1} 3300, 3050, 1608, 1493, 1443 and 1217; ^1H NMR (300 MHz; $\text{DMSO-}d_6$) δ_{H} 7.50 (2H, t, $^3J = 9.0$ Hz), 7.86 (2H, dd, $^3J = 6.6$ Hz, $^4J = 3.3$ Hz), 8.20 (2H, dd, $^3J = 6.6$ Hz, $^4J = 3.3$ Hz), 8.35 (2H, s), 8.41 (2H, dd, $^3J = 8.8$ Hz, $^4J = 3.3$ Hz), 13.39 (1H, s) ppm; ^{13}C NMR (75 MHz; $\text{DMSO-}d_6$) δ_{C} 116.40 (d, $J_{\text{CF}} = 22.1$ Hz), 125.45 (d, $J_{\text{CF}} = 3.1$ Hz), 126.58, 128.91, 129.71, 130.31 (d, $J_{\text{CF}} = 9.1$ Hz), 140.02, 141.77, 158.65, 162.57, 165.89, 166.35 ppm; Anal. Calcd for $\text{C}_{19}\text{H}_{11}\text{FN}_4$: C, 72.60; H, 3.53; N, 17.82. Found: C, 72.73; H, 3.65; N, 17.93.

2.1.2.3. 3-(1*H*-Imidazo[4,5-*b*]phenazin-2-yl)phenol (4c)

Workup gave **4c** as a brown powder; yield = 42%; mp > 300 °C; $\tilde{\nu}_{\text{max}}$ (atr)/ cm^{-1} 3350, 3015, 1599, 1531, 1492, 1449, and 1217; ^1H NMR (300 MHz; $\text{DMSO-}d_6$) δ_{H} 7.04 (1H, dd, $^3J = 8.1$ Hz, $^4J = 1.5$ Hz), 7.44 (1H, t, $^3J = 8.1$ Hz), 7.77–7.78 (2H, m), 7.86 (2H, dd, $^3J = 6.9$ Hz, $^4J = 3.3$ Hz), 8.21 (2H, dd, $^3J = 6.6$ Hz, $^4J = 3.6$ Hz), 8.47 (1H, br.), 9.93 (1H, s), 13.33 (1H, s), 13.43 ppm (1H, br.); Anal. Calcd for $\text{C}_{19}\text{H}_{12}\text{N}_4\text{O}$: C, 73.07; H, 3.87; N, 17.94. Found: C, 73.22; H, 3.95; N, 17.82.

2.1.2.4. 4-(1*H*-Imidazo[4,5-*b*]phenazin-2-yl)phenol (4d)

Workup gave **4d** (CAS No. 303059-19-0) as a brown powder; yield = 82 %; mp > 300 °C; ^1H NMR (300 MHz; $\text{DMSO-}d_6$) δ_{H} 6.68 (1H, d, $^3J = 8.3$ Hz), 7.00 (2H, d, $^3J = 8.6$ Hz), 7.04 (1H, d, $J = 8.5$ Hz), 7.85 (2H, dd, $^3J = 6.6$ Hz, $^4J = 3.3$ Hz), 8.18–8.23 (4H, m), 9.26 (1H, br.), 13.16 ppm (1H, br.); ^{13}C NMR (75 MHz; $\text{DMSO-}d_6$) δ_{C} 114.81, 116.03, 119.51, 128.85, 129.43, 129.82, 129.96, 140.15, 141.58, 156.27, 160.05, 161.04 ppm; Anal. Calcd for $\text{C}_{19}\text{H}_{12}\text{N}_4\text{O}$: C, 73.07; H, 3.87; N, 17.94. Found: C, 73.12; H, 3.93; N, 18.10.

2.1.2.5. 2-(4-(Benzyloxy)phenyl)-1*H*-imidazo[4,5-*b*]phenazine (4e)

Workup gave **4e** as a brown powder; yield = 81 %; mp > 300 °C; ^1H NMR (400 MHz; $\text{DMSO-}d_6$) δ_{H}

5.25 (2H, s), 7.29 (2H, d like, $^3J = 9.0$ Hz), 7.34-7.38 (1H, m), 7.40-7.44 (2H, m), 7.50 (2H, d like, $^3J = 7.2$ Hz), 7.86 (2H, dd, $^3J = 6.8$ Hz, $^4J = 3.2$ Hz), 8.19-8.21 (3H, m), 8.32 (2H, d, $^3J = 8.8$ Hz), 8.41 (1H, s), 13.27 ppm (1H, s); ^{13}C NMR (100 MHz; DMSO- d_6) δ_{C} 69.62, 115.57, 121.32, 127.92, 128.12, 128.59, 128.88, 129.70, 136.60, 141.71, 159.67, 161.40 ppm; Anal. Calcd for $\text{C}_{26}\text{H}_{18}\text{N}_4\text{O}$: C, 77.59; H, 4.51; N, 13.92. Found: C, 77.65; H, 4.70; N, 13.78.

2.1.2.6. 4-(1*H*-Imidazo[4,5-*b*]phenazin-2-yl)-2-methoxyphenol (4f)

Workup gave **4f** (CAS No. 114991-90-1) as a brown powder; yield = 76%; mp > 300 °C; ^1H NMR (400 MHz; DMSO- d_6) δ_{H} of 3.94 (3H, s), 7.01 (1H, d, $^3J = 8.0$ Hz), 7.41 (1H, dd, $^3J = 8.0$ Hz, $^4J = 2.0$ Hz), 7.73 (1H, d, $^4J = 2.0$ Hz), 7.86-7.87 (2H, m), 8.20-8.22 (2H, m), 8.39 (1H, s), 9.76 (1H, s), 12.63 (s, 1H), 13.19 ppm (s, 1H); Anal. Calcd for $\text{C}_{20}\text{H}_{14}\text{N}_4\text{O}_2$: C, 70.17; H, 4.12; N, 16.37. Found: C, 70.22; H, 4.23; N, 16.46.

2.1.2.7. 2-(4-(Benzyloxy)-3-methoxyphenyl)-1*H*-imidazo[4,5-*b*]phenazine (4g)

Workup gave **4g** as a brown powder; yield = 79%; mp > 300 °C; ^1H NMR (400 MHz; DMSO- d_6) δ_{H} 3.95 (3H, s), 5.23 (2H, s), 7.32-7.43 (5H, m), 7.49-7.51 (2H, m), 7.86-7.88 (2H, m), 7.94-7.97 (2H, m), 8.20-8.23 (2H, m), 8.43 (1H, s), 13.27 ppm (1H, s); Anal. Calcd for $\text{C}_{27}\text{H}_{20}\text{N}_4\text{O}_2$: C, 74.98; H, 4.66; N, 12.95. Found: C, 75.11; H, 4.72; N, 12.82.

2.1.2.8. 2-(2,5-Dimethoxyphenyl)-1*H*-imidazo[4,5-*b*]phenazine (4h)

Workup gave **4h** as a brown powder; yield = 35%; mp > 300 °C; ^1H NMR (300 MHz; DMSO- d_6) δ_{H} 3.85 (3H, s), 4.06 (3H, s), 7.20 (1H, dd, $^3J = 9.0$ Hz, $^4J = 3.3$ Hz), 7.28 (1H, d, $^3J = 9.3$ Hz), 7.86 (2H, dd, $^3J = 6.6$ Hz, $^4J = 3.3$ Hz), 8.02 (1H, d, $^4J = 3.0$ Hz), 8.22 (2H, dd, $^3J = 6.9$ Hz, $^4J = 3.6$ Hz), 8.35 (1H, s), 8.47 (1H, s), 12.51 (1H, s) ppm; ^{13}C NMR (75 MHz; DMSO- d_6) δ_{C} 55.65, 56.41, 106.75, 113.91, 114.13, 116.93, 119.88, 128.86, 128.97, 129.48, 129.70, 139.82, 140.04, 140.42, 141.69, 141.81, 147.62, 152.36, 153.22, 157.32 ppm; Anal. Calcd for $\text{C}_{21}\text{H}_{16}\text{N}_4\text{O}_2$: C, 70.77; H, 4.53; N, 15.72. Found: C, 70.83; H, 4.65; N, 15.92.

2.1.2.9. 2-(5-Methylfuran-2-yl)-1*H*-imidazo[4,5-*b*]phenazine (4i)

Workup gave **4i** as a reddish brown powder; yield = 61%; mp > 300 °C; $\tilde{\nu}_{\text{max}}$ (atr)/ cm^{-1} 3370, 3052, 1623, 1557, 1419, 1345 and 1212; ^1H NMR (300 MHz; DMSO- d_6) δ_{H} 2.50 (3H, s), 6.50 (1H, d, $^3J =$

2.7 Hz), 7.47 (1H, d, $^3J = 3.3$ Hz), 7.87 (2H, dd, $^3J = 6.6$ Hz, $^4J = 3.3$ Hz), 8.16 (1H, s), 8.21 (2H, br.), 8.38 (1H, s), 13.28 (1H, s) ppm; ^{13}C NMR (75 MHz; DMSO- d_6) δ_{C} 13.66, 105.56, 109.62, 114.08, 116.38, 128.81, 128.96, 140.01, 151.22, 156.55 ppm; Anal. Calcd for $\text{C}_{18}\text{H}_{12}\text{N}_4\text{O}$: C, 71.99; H, 4.03; N, 18.66. Found: C, 72.15; H, 4.11; N, 18.73.

2.1.2.10. 2-(Pyridin-3-yl)-1*H*-imidazo[4,5-*b*]phenazine (4j)

Workup gave **4j** as a brown powder; yield = 24%; mp > 300 °C; ^1H NMR (300 MHz; DMSO- d_6) δ_{H} 7.59 (1H, t like, $^3J = 5.4$ Hz), 7.79 (2H, dd, $^3J = 6.9$ Hz, $^4J = 3.3$ Hz), 8.16 (2H, dd, $^3J = 6.9$ Hz, $^4J = 3.6$ Hz), 8.31 (2H, s), 8.70 (1H, s), 8.72 (1H, t like, $^3J = 5.3$ Hz), 9.55 ppm (1H, s); ^{13}C NMR (75 MHz; DMSO- d_6) δ_{C} 106.02, 109.98, 123.94, 127.57, 128.81, 135.08, 139.79, 141.25, 148.53, 148.91, 151.17 ppm; Anal. Calcd for $\text{C}_{18}\text{H}_{11}\text{N}_5$: C, 72.72; H, 3.73; N, 23.56. Found: C, 72.88; H, 3.82; N, 23.66.

2.1.3. General Procedure II for the synthesis of 1-substituted imidazo[4,5-*b*]phenazine 6a-d

A mixture of **4a** or **4i** (5 mmol), methyl bromoacetate (**5a**) (5 mmol) or ethyl bromoacetate (**5b**) (5 mmol) and anhydrous K_2CO_3 (0.69 g, 5 mmol) was stirred under reflux in acetone (25 mL) for 4 h. After cooling to rt the mixture was poured in ice-water and the precipitated products were filtered, dried and purified by flash chromatography (Pet. Ether / EtOAc 1:1.5 to EtOAc / MeOH 1: 0.05) to afford **6a-d**.

2.1.3.1. Methyl 2-(2-(*p*-tolyl)-1*H*-imidazo[4,5-*b*]phenazin-1-yl)acetate (6a)

Workup gave **6a** as a reddish brown powder; yield = 72%; mp > 300 °C; ^1H NMR (400 MHz; DMSO- d_6) δ_{H} 2.44 (3H, s), 3.69 (3H, s), 5.43 (2H, s), 7.45 (2H, d, $^3J = 8.0$ Hz), 7.77 (2H, d, $^3J = 8.4$ Hz), 7.89-7.91 (2H, m), 8.21-8.26 (2H, m), 8.45 (1H, s), 8.54 (1H, s) ppm; Anal. Calcd for $\text{C}_{23}\text{H}_{18}\text{N}_4\text{O}_2$: C, 72.24; H, 4.74; N, 14.65. Found: C, 72.37; H, 4.82; N, 14.73.

2.1.3.2. Ethyl 2-(2-(*p*-tolyl)-1*H*-imidazo[4,5-*b*]phenazin-1-yl)acetate (6b)

Workup gave **6b** as a reddish brown powder; yield = 74%; mp > 300 °C; ^1H NMR (400 MHz; DMSO- d_6) δ_{H} 1.25 (3H, t, $^3J = 7.0$ Hz), 2.47 (3H, s), 4.40 (2H, q, $^3J = 7.0$ Hz), 5.55 (2H, s), 7.47 (2H, d, $^3J = 8.0$ Hz), 7.86 (2H, dd, $^3J = 6.8$ Hz, $^4J = 3.3$ Hz), 7.89 (2H, d, $^3J = 8.0$ Hz), 7.96 (2H, d, $^3J = 8.0$ Hz), 8.25 (1H, s), 8.45 (1H, s) ppm; Anal. Calcd for $\text{C}_{24}\text{H}_{20}\text{N}_4\text{O}_2$: C, 72.71; H, 5.09; N, 14.13. Found: C, 72.81; H, 5.21; N, 14.26.

2.1.3.3. Methyl 2-(2-(5-methylfuran-2-yl)-1H-imidazo[4,5-b]phenazin-1-yl)acetate (6c)

Workup gave **6c** as a reddish brown powder; yield = 46%; mp > 300 °C; ¹H NMR (400 MHz; DMSO-*d*₆) δ_H 2.49 (3H, ov.), 3.83 (3H, s), 5.37 (2H, s), 6.32 (1H, d, ⁴*J* = 2.8 Hz), 7.45 (1H, d, ³*J* = 3.2 Hz), 7.81 (2H, dd, ³*J* = 6.8 Hz, ⁴*J* = 3.2 Hz), 8.04 (1H, s), 8.22 (1H, dd, ³*J* = 6.8 Hz, ⁴*J* = 3.6 Hz), 8.28 (1H, dd, ³*J* = 6.4 Hz, ⁴*J* = 3.6 Hz), 8.63 (1H, s) ppm; Anal. Calcd for C₂₁H₁₆N₄O₃: C, 67.73; H, 4.33; N, 15.05. Found: C, 67.82; H, 4.45; N, 15.12.

2.1.3.4. Ethyl 2-(2-(5-methylfuran-2-yl)-1H-imidazo[4,5-b]phenazin-1-yl)acetate (6d)

Workup gave **6d** as a reddish brown powder; yield = 53 %; mp > 300 °C; ν_{max} (atr)/cm⁻¹ 2991, 1742, 1608, 1576, 1547, 1493, 1422, and 1209; ¹H NMR (300 MHz; DMSO-*d*₆) δ_H 1.22 (3H, t, ³*J* = 7.0 Hz), 2.43 (3H, s), 4.25 (2H, q, ³*J* = 7.0 Hz), 5.63 (2H, s), 6.51 (1H, d, ³*J* = 2.7 Hz), 7.48 (1H, d, ³*J* = 2.7 Hz), 7.88 (1H, dd, ³*J* = 6.7 Hz, ⁴*J* = 3.4 Hz), 8.19-8.24 (3H, m), 8.43 (1H, s), 8.50 (1H, s) ppm; Anal. Calcd for C₂₂H₁₈N₄O₃: C, 68.38; H, 4.70; N, 14.50. Found: C, 68.47; H, 4.78; N, 14.61.

2.2. Biology

2.2.1. *In vitro* antiproliferative activity against a panel of 60 cell lines

The growth inhibitory assay against 60 cell line panel was done for all the imidazophenazines **4a-j** and **6a-d** at the National Cancer Institute (NCI), Bethesda, Maryland, USA.

2.2.2. Anticancer activity against MCF-7 cell line

The anticancer activity of **4f** on MCF-7 was done at the National Cancer Institute (NCI) - Cairo - Egypt, applying SRB assay according to the reported procedure and the results were compared with etoposide and camptothecin as standards (for further details see the SI) [39].

2.2.3. Topo I mediated DNA relaxation assay

Compounds **4a** and **4e-g** were investigated for their ability to inhibit Topo I DNA relaxation using a Topo I assay kit from Topogen (USA) and camptothecin was utilized as a standard. The Topo I assay was carried out according to manufacturer's instructions (For further details see SI) [40].

2.2.4. Topo II α (TopoGene) mediated DNA relaxation assay

Compounds **4a** and **4e-g** were also investigated for their ability to inhibit Topo II α DNA relaxation and etoposide was used as a standard. The Topo II α

assay was done according to manufacturer's instructions (For further details see SI) [41].

2.2.5. Cell Cycle Analysis Assay

Cell cycle analysis was performed in MCF-7 cells for compound **4f** to determine its effect on cell cycle distribution via flow cytometry. The assay was performed according to manufacturer's instructions (For further details see SI) [42].

2.2.6. Annexin V-APC/7-AAD Apoptosis Detection

Annexin V apoptosis assay was done in MCF-7 cells for compound **4f** to determine its effect of on induction of apoptosis via flow cytometry. The assay was performed according to manufacturer's instructions (For further details see SI) [42].

2.3. Molecular docking

Molecular docking simulations were done using Molecular Operating Environment (MOE, 2022.02) software. The X-ray crystallographic structure of human topoisomerase I in complex with DNA and camptothecin (PDB ID: 1T8I) [43], and human topoisomerase II α in complex with DNA and etoposide (PDB ID: 5GWK) [11] were used in this study. The details of the molecular docking simulation methodology are described in details in the supporting materials.

2.4. Estimation of physicochemical, pharmacokinetic and ADME properties

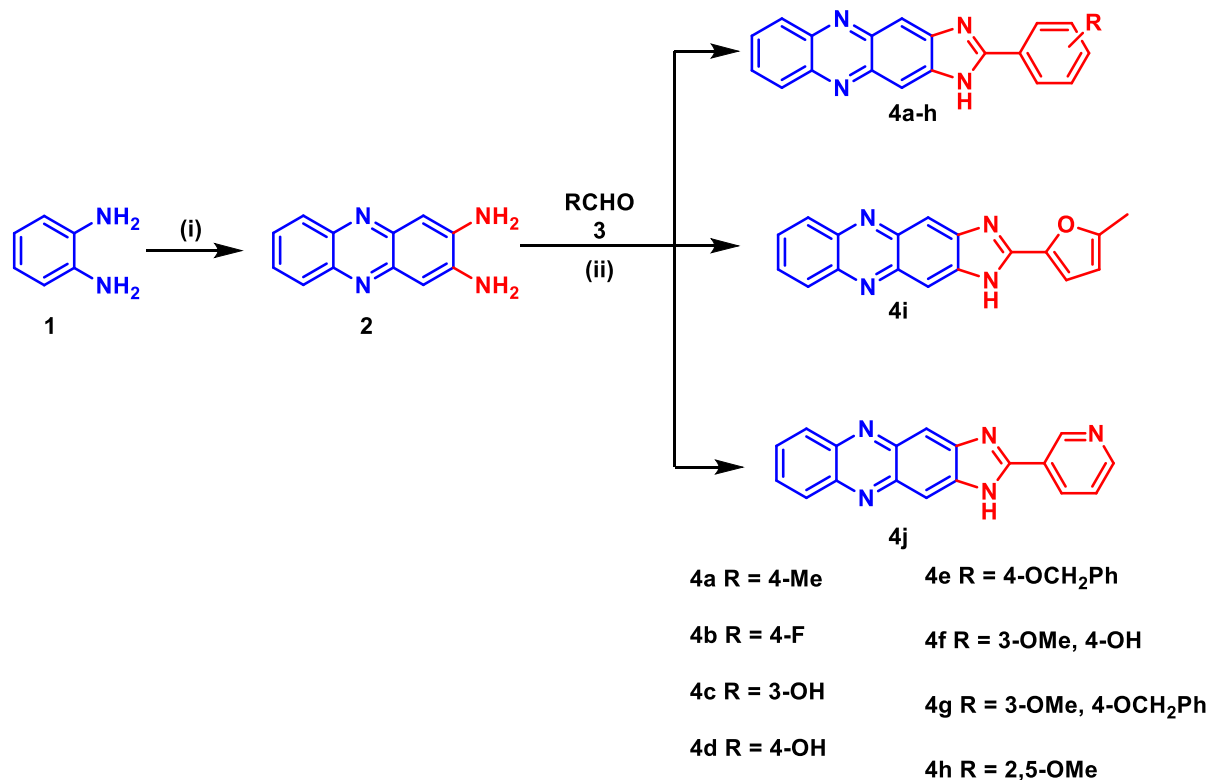
Calculation of the physicochemical descriptors to predict the ADME parameters, and pharmacokinetic properties of the most promising compounds was performed utilizing SwissADME web tool available from the Swiss Institute of Bioinformatics (SIB) [44].

3. Results and discussion

3.1. Chemistry

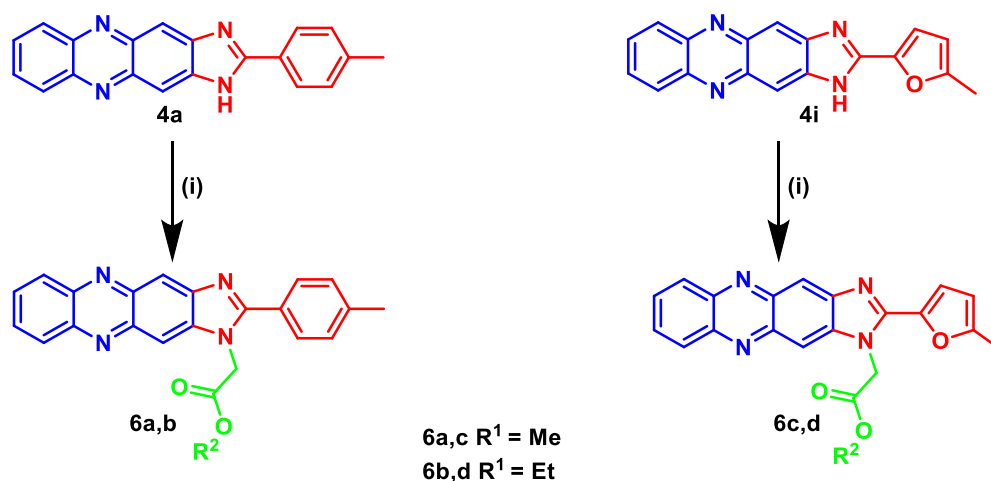
Initially, 1,2-phenylenediamine (**1**) was treated with catalytic amounts of ceric ammonium nitrate at r.t. in aqueous conditions to give phenazine-2,3-diamine (**2**). Condensation of **2** with aromatic as well as heterocyclic aldehydes **3** were simply carried out in DMF in the presence of catalytic amounts of glacial acetic acid to afford the target imidazo[4,5-*b*]phenazines **4** in excellent yields (Scheme 1). Different spectroscopic measurements as well as elemental analysis were carried out to for structural elucidation of **4a-j**.

Compounds **4a** and **4i** were further reacted with methyl bromoacetate (**5a**) and ethyl bromoacetate (**5b**) in acetone under basic conditions to give **6a-d**, respectively (Scheme 2).



Reagents and conditions: (i) CAN, acetone / water (1:1), rt, 96h; (ii) gl. acetic acid, DMF, reflux, 4h

Scheme 1: Synthesis of 2-substituted imidazo[4,5-*b*]phenazines **4a-j**



Reagents and conditions: (i) BrCH₂COOMe (5a), BrCH₂COOEt (5b), anhydrous K₂CO₃, acetone, reflux, 4 h

Scheme 2: Synthesis of 1,2-disubstitued-1*H*-imidazo[4,5-*b*]phenazine **6a-d**

3.2. Biological evaluation

3.2.1. *In vitro* single dose (10 μ M) anticancer assay on NCI 60 cell panel

All the imidazophenazines **4a-j** and **6a-d** were *in vitro* evaluated in NCI, USA at a single dose (10⁻⁵ M) level on different NCI cell panel. The growth inhibition percent (GI%) of the treated cells

compared to the untreated control cells were depicted in Table 1.

Analysis of the obtained results showed that the tested imidazo[4,5-*b*]phenazine based compounds have a distinctive pattern of selectivity against different NCI cell panel. The tested compounds inhibited the growth of at least one cancer cell line. In

the leukemia sub-panel, several cell lines showed a reasonable sensitivity to most of the tested compounds such as K-562, MOLT-4, and SR cell lines with GI% ranges of 11-44%, 10-82%, and 11-44%, respectively. In the non-small cell lung cancer sub-panel, HOP-92, NCI-H23, NCI-H522 cell lines showed a reasonable sensitivity to most of the tested compounds with GI% ranges of 14-52%, 14-30%, and 10-33%, respectively. In the colon cancer sub-panel, HCT-116 cell line showed a reasonable sensitivity to most of the tested compounds with a GI% range of 11-33%. In the CNS cancer sub-panel, SNB-75 cell line showed a reasonable sensitivity to some of the tested compounds with a GI% range of 12-30%. In the ovarian cancer sub-panel, OVCAR-8 and SK-OV-3 cell lines showed a reasonable sensitivity to most of the tested compounds with GI% ranges of 10-40% and 12-88%, respectively. In the renal cancer sub-panel, UO-31 cell line showed a reasonable sensitivity to most of the tested compounds with a GI% range of 13-54%. PC-3 cell lines in the prostate cancer sub-panel showed a

reasonable sensitivity to most of the tested compounds with a GI% range of 12-27%. In the breast cancer sub-panel, MCF-7, MDA-MB-231, BT-549, T-47D, and MDA-MB-468 showed a reasonable sensitivity to most of the tested compounds with GI% ranges of 13-66%, 12-41%, 10-37, 14-48% and 10-33%, respectively.

The imidazophenazine **4f** revealed a potent and broad spectrum anticancer activity against the tested cancer cell lines. It showed more than 50% growth inhibition against CCRF-CEM and MOLT-4 cell lines from leukaemia sub-panel, HOP-92 and NCI-H460 cell lines from non-small cell lung cancer sub-panel, UO-31 cell line from renal cancer sub-panel, and MCF-7 cell line from breast cancer sub-panel (**Table 1** and **Fig. 5**). Furthermore, compound **4b** showed more than 50% growth inhibition against M14 cell line from melanoma sub-panel, whereas compound **4e** revealed more than 50% growth inhibition against Sk-OV-3 cell line from ovarian cancer sub-panel.

Table 1. Growth inhibition % (GI %) of the target compounds **4a-4j** and **6a-d** *in vitro* against a panel of tumor cell lines at 10 μ M

Subpanel	Compound ID													
	4a	4b	4c	4d	4e	4f	4g	4h	4i	4j	6a	6b	6c	6d
	GI %													
Leukemia														
CCRF-CEM	- ^a	-	22	27	-	66	-	-	10	-	-	-	-	-
HL-60(TB)	-	21	12	13	-	20	-	-	15	18	-	-	-	-
K-562	-	13	18	19	15	44	19	-	-	11	27	14	-	17
MOLT-4	-	-	18	25	14	82	-	-	-	-	30	10	-	-
PRMI-8226	-	-	24	21	-	46	-	-	-	-	11	-	-	-
SR	-	11	23	31	13	44	11	-	-	-	29	15	-	-
Non-small cell lung Cancer														
A549/ATTC	-	-	20	-	-	37	-	-	-	-	14	-	-	-
EKVX	12	-	-	-	-	-	-	10	31	-	-	-	-	-
HOP-62	14	-	-	-	19	28	18	17	-	-	-	-	-	-
HOP-92	-	-	-	16	16	52	14	-	-	14	20	26	-	-
NCI-H226	-	-	-	-	-	23	-	-	12	-	-	-	-	-
NCI-H23	-	-	-	-	15	30	17	14	15	-	22	-	-	-
NCI-H322M	-	-	-	-	-	12	-	-	-	-	11	-	-	-
NCI-H460	-	-	-	-	-	60	-	-	-	-	-	-	-	-
NCI-H522	13	33	12	10	-	28	-	30	-	-	22	-	-	-
Colon Cancer														
COLO 205	-	-	-	-	-	-	-	-	-	-	-	-	-	-
HCC-2998	-	-	-	-	-	-	-	-	-	-	-	-	-	-
HCT-116	13	30	13	-	11	23	-	33	-	22	-	-	-	-
HCT-15	-	-	-	-	11	29	-	-	-	-	-	-	-	-
HT29	-	-	19	-	-	-	-	-	-	-	-	-	-	-
KM12	-	-	25	-	-	27	-	-	-	-	-	-	-	-
SW-620	-	-	-	-	-	25	-	-	-	-	-	-	-	-
CNS Cancer														
SF-268	-	-	12	-	-	16	-	-	-	-	-	-	-	-
SF-295	-	-	-	-	-	14	-	-	-	-	-	-	-	-

SF-539	-	-	19	16	-	15	-	-	-	-	-	-	-
SNB-19	-	-	-	-	-	19	-	-	-	-	-	-	-
SNB-75	-	-	12	-	-	24	-	-	17	15	30	-	-
U251	-	-	-	-	-	19	-	-	-	-	-	-	-
Melanoma													
LOX IMVI	-	-	-	13	-	33	13	-	15	-	-	-	-
MALME-3M	-	-	-	-	-	-	-	-	-	-	-	-	-
M14	-	51	-	-	-	-	-	10	-	-	-	-	-
MDA-MB-435	-	-	-	-	-	11	-	-	-	-	-	-	-
SK-MEL-2	-	-	-	-	-	-	-	13	-	-	-	-	11 14
SK-MEL-28	-	-	-	-	-	-	-	-	-	-	-	-	-
SK-MEL-5	-	-	20	-	-	41	-	-	-	16	24	-	-
UACC-257	-	-	-	-	-	-	-	-	-	-	-	-	-
UACC-62	-	-	-	-	-	23	-	-	-	-	-	-	-
Ovarian Cancer													
IGROV1	-	-	-	-	-	31	-	13	-	-	16	-	-
OVCAR-3	-	38	-	-	-	20	-	-	-	-	16	-	-
OVCAR-4	-	-	-	-	-	18	-	-	12	-	27	-	-
OVCAR-5	-	-	-	-	-	-	-	-	-	-	-	-	-
OVCAR-8	-	27	13	-	-	40	-	-	11	12	10	-	-
NCI/ADR-RES	-	-	-	-	-	-	-	-	-	-	-	-	-
SK-OV-3	-	-	-	-	88	15	19	20	12	-	-	-	-
Renal Cancer													
786-0	-	-	14	-	-	11	-	-	-	-	-	-	-
A498	-	-	-	-	-	18	-	-	-	-	20	-	-
ACHN	-	-	-	16	-	43	11	-	-	-	-	-	-
CAKI-1	-	-	-	-	-	42	16	-	-	-	-	-	-
RXF 393	-	-	-	-	-	13	-	-	-	-	-	-	-
SN 12C	-	-	-	-	-	26	-	-	-	-	-	-	-
TK-10	-	-	-	-	-	-	-	-	-	-	-	-	-
UO-31	37	-	20	26	30	54	31	13	25	20	28	-	-
Prostate Cancer													
PC-3	-	-	16	15	-	27	12	14	14	25	13	-	-
DU-145	-	-	-	-	-	17	-	-	-	-	17	-	-
Breast Cancer													
MCF-7	-	15	29	29	30	66	38	28	-	25	-	-	13 -
MDA-MB-231/ATTC	30	-	-	16	12	41	19	22	-	-	-	-	-
HS 578T	-	-	-	-	10	13	-	-	-	-	-	-	-
BT-549	-	14	37	10	-	-	-	-	-	12	19	-	-
T-47D	30	38	25	14	33	48	25	-	-	18	44	-	-
MDA-MB-468	33	10	-	-	-	25	-	-	-	10	-	-	-

^a: GI% < 10%.

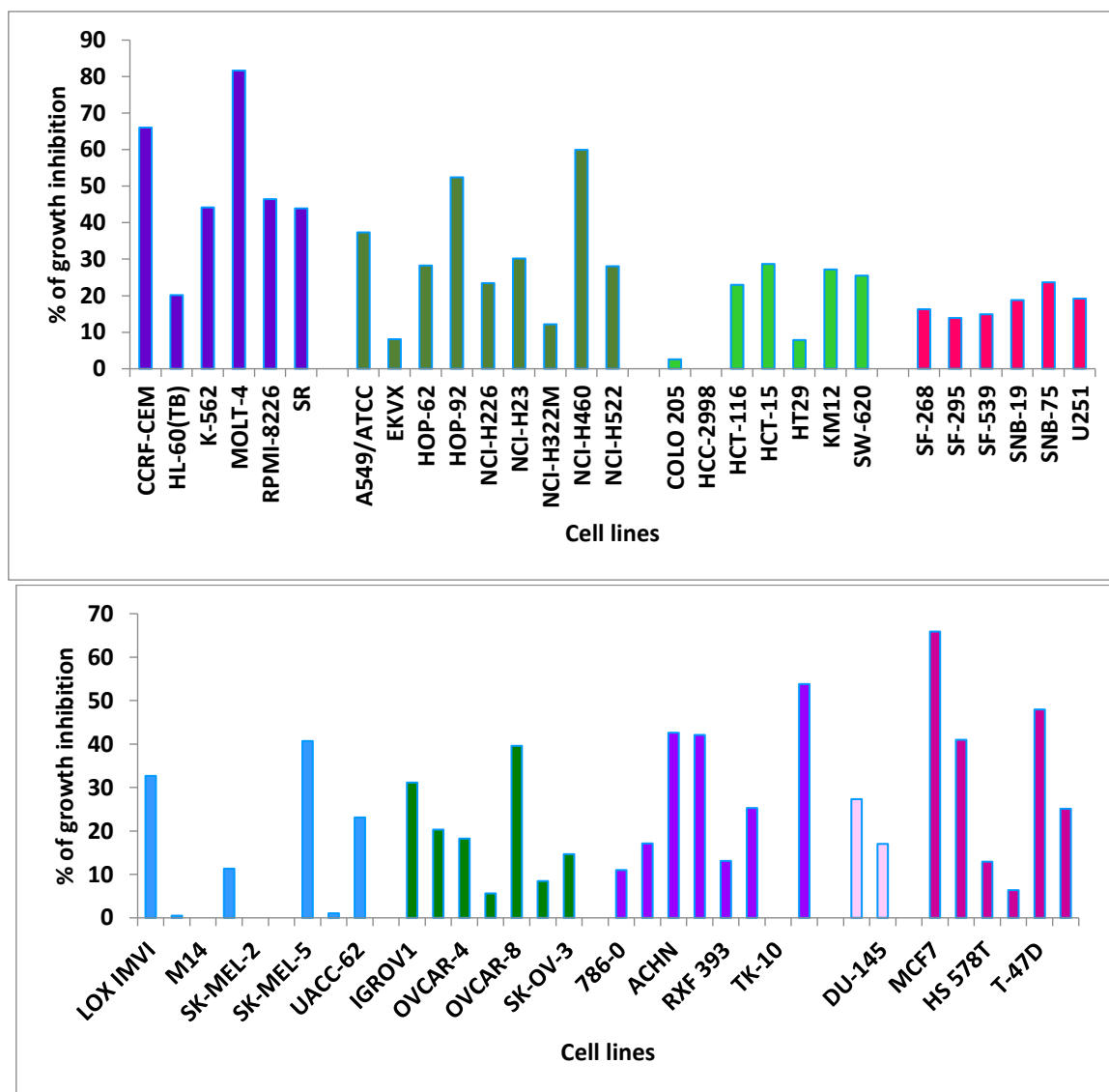


Fig. 5: Growth inhibition % (GI%) of NCI cancer cell lines after treatment with 10 μ M of compound **4f**

3.2.2. *In vitro* antiproliferative activity of **4f** against MCF-7

Based on the results of NCI, the imidazophenazine **4f** was selected to be evaluated for its growth inhibitory activity on MCF-7 cell line via the Sulfo-Rhodamine-B (SRB) assay and its IC_{50} (μ M) value was compared to etoposide and camptothecin (Table 2). The imidazophenazine derivative **4f** was found to possess comparable anticancer activity against MCF-7 breast cancer cell line (IC_{50} = 16.3 μ M) to etoposide (IC_{50} = 15.1 μ M).

Table 2: Anticancer activity of **4f** against MCF-7 cancer cell line

Compound ID	IC_{50} (μ M)
4f	16.3
Camptothecin (I)	28.7
Etoposide (III)	15.1

3.2.3. Topoisomerase I and II α Inhibitory activity of **4a** and **4e-g**

The most potent phenazines **4a** and **4e-g** were evaluated for their ability to inhibit conversion of the supercoiled plasmid DNA to relaxed DNA by recombinant topoisomerase I and II α and were compared to the reference standards camptothecin (as topo I inhibitor) and etoposide (as topo II inhibitor). The reaction products of topoisomerase I and II α relaxation assays were analyzed at (100, 50, 25 and 13 μ M) by electrophoretic mobility, and developed in ethidium bromide in the presence of UV light. The IC_{50} results were depicted in table 3.

From the obtained results, it is obvious that the tested compounds revealed moderate to potent dual topo I and topo II α inhibitory activity in comparison to the positive controls camptothecin and etoposide, respectively. Compound **4e** was found to be the most

potent against Topo I ($IC_{50} = 29.25 \mu M$) in comparison to camptothecin ($IC_{50} = 25.71 \mu M$), whereas compounds **4a**, **4f** and **4g** ($IC_{50} = 43.52 - 48.28 \mu M$) demonstrated moderate potency in comparison to camptothecin ($IC_{50} = 25.71 \mu M$). Compounds **4f** ($IC_{50} = 26.74 \mu M$) and **4g** ($IC_{50} = 22.72 \mu M$) displayed comparable potency to etoposide ($IC_{50} = 20.52 \mu M$) against Topo II α , whereas compounds **4a** and **4e** showed slightly less potent activity ($IC_{50} = 33.27$ and $37.06 \mu M$, respectively).

Table 3. Inhibitory activity of selected imidazophenazines **4a** and **4e-g** as well as the reference standards on Topo I and Topo II α

Compound ID	IC_{50} (μM) ^a	
	Topo I	Topo II α
4a	46.11 \pm 3.2	33.27 \pm 2.5
4e	29.25 \pm 2.7	37.06 \pm 2.6
4f	48.28 \pm 3.6	26.74 \pm 3.1
4g	43.52 \pm 3.1	22.72 \pm 1.9
Camptothecin	25.71 \pm 1.9	-
Etoposide	-	20.52 \pm 1.3

^a: The concentrations of the inhibitor that prevented 50% of the supercoiled DNA from being converted into relaxed DNA (IC_{50} values)

3.2.4. Cell cycle analysis of MCF-7 cell line after treatment with **4f**

The effect of **4f** at its IC_{50} on MCF-7 cell cycle progression was investigated by staining the MCF-7 cells with PI (propidium iodide) and employing flow cytometry. The cell cycle profile of MCF-7 cells without and with **4f** treatment for 24 h was depicted in **Fig. 6**. It is interesting to find that the fraction of G1 phase was decreased from 75.34% in control cells to 70.00% in **4f** treated cells. In addition, the percentage of cells accumulated in G2 phase was increased from 0.17 % in untreated cells to 5.50% in **4f** treated cells. This result indicated that compound **4f** arrested MCF-7 cells in the G2/M phase of the cell cycle by 5.33%.

3.2.5. Evaluation of the effect of **4f** on the apoptosis of MCF-7 cell line

Compound **4f** was further evaluated for its ability to induce apoptosis in MCF-7 cell line. **Fig. 7** displayed the apoptosis of MCF-7 cells before and after **4f** treatment at its IC_{50} . It is interesting to find that **4f** induces apoptosis in MCF-7 cell lines as the percentage of cells in the early apoptotic, late apoptotic, and necrotic stages was increased from 5.12, 7.57, 1.77 %, respectively, in control cells to 12.22, 11.29 and 3.61%, respectively, in **4f** treated MCF-7 cells.

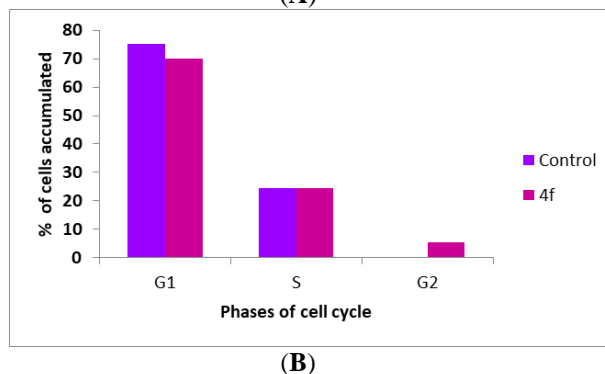
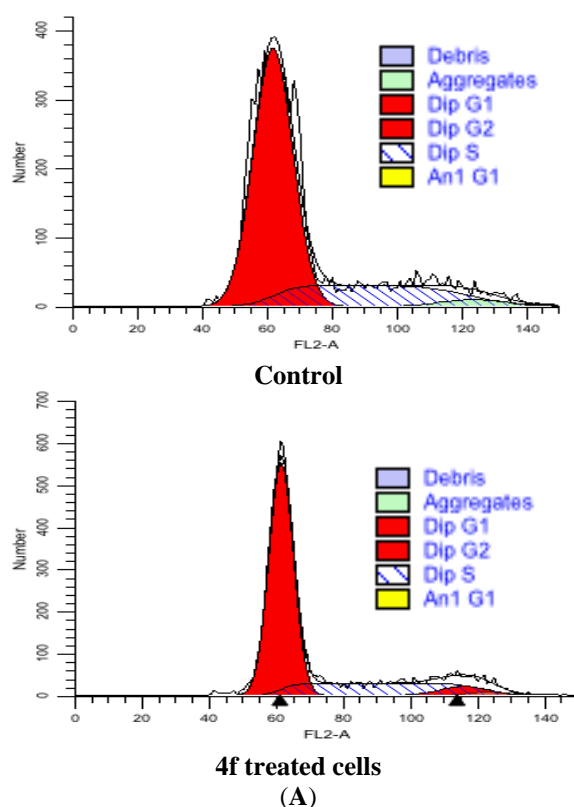


Fig. 6: Analysis of MCF-7 cell cycle before and after treatment with **4f**

3.3. Molecular docking study

To study the plausible binding pattern of the promising compounds **4a**, **4e-g** in the target topoisomerase I and II α , molecular docking simulations were utilized. For the intended molecular docking study, the X-ray crystallographic structure of human topoisomerase I in complex with DNA and camptothecin (PDB ID: 1T8I) and human topoisomerase II α in complex with DNA and etoposide (PDB ID: 5GWK) were downloaded from the protein data bank [11, 43]. The co-crystallized topoisomerases' poisons slide by their polycyclic scaffold in the DNA cleavage site physically interfering with the stacking base pairs (DNA intercalation) what successfully halts and stabilizes the topoisomerase/DNA cleavage complex preventing the re-ligation reaction [11, 12].

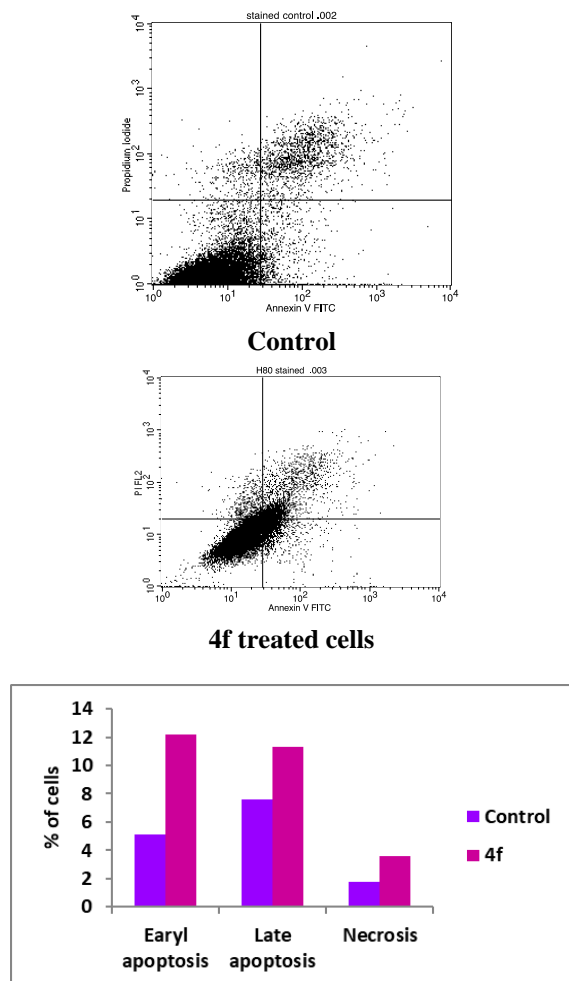
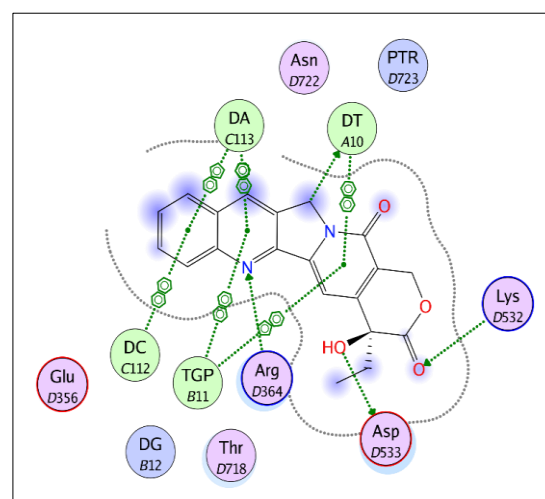


Fig. 7: Apoptosis inducing effect of **4f** on MCF-7 cell line

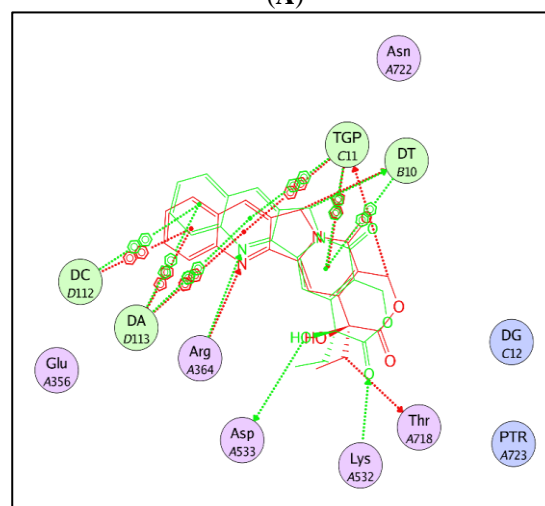
Initially, the adopted molecular docking setup was validated by self-docking of the complexed ligands (camptothecin & etoposide) in the vicinity of their binding site in the target enzymes. The self-docking validation step revealed the aptness of the utilized docking protocols for the proposed molecular docking simulation by the small RMSD value between the docking and complexed ligands' poses (**Table 4**) and by the ability of the docking poses of the complexed ligands to replicate all the key interactions achieved by the complexed ligands (**Fig. 8** and **9**).

Table 4. RMSD (Å) and docking score (kcal/mol) of the co-crystallized ligands in the self-docking validation step

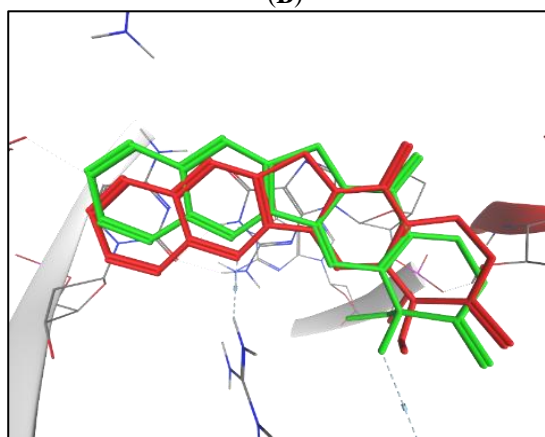
PDB: ID	Co-crystallized ligand	RMSD (Å)	Docking Score (S) kcal/mol
1T8I	Camptothecin	0.781	-13.24
5GWK	Etoposide	1.825	-15.75



(A)

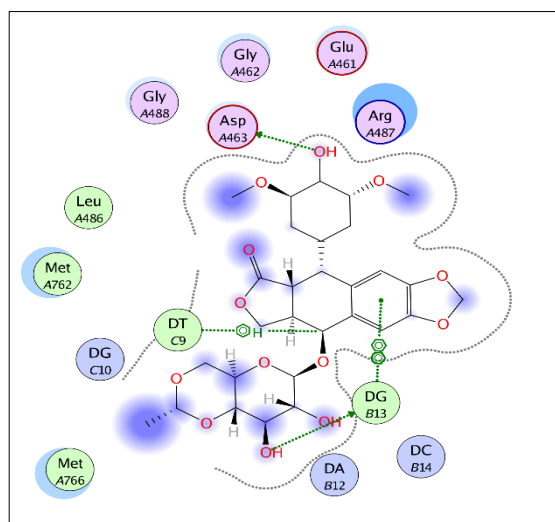


(B)

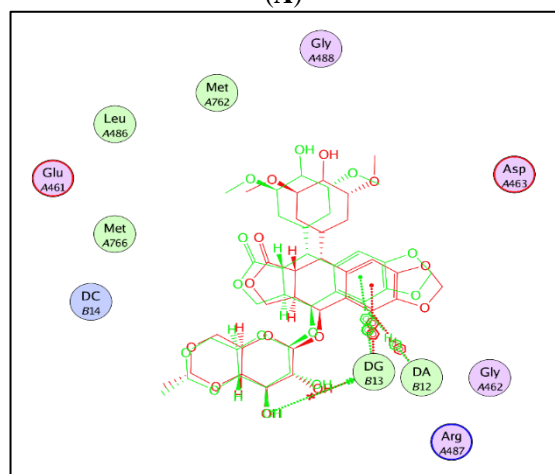


(C)

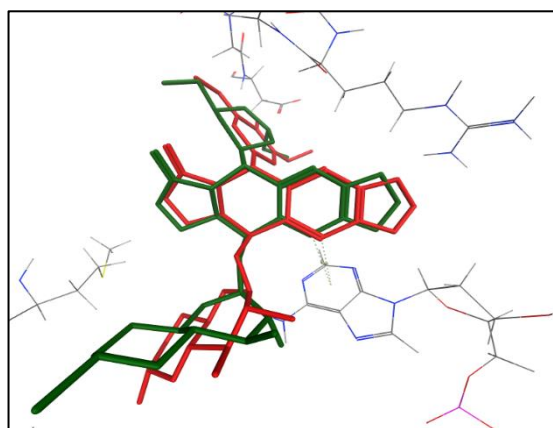
Fig. 8: (A) 2D interaction diagram showing camptothecin docking pose key interactions in topoisomerase I binding site. (B) 2D diagram and (C) 3D representation showing the superimposition of the co-crystallized (red) and the docking pose (green) of camptothecin in topoisomerase I binding site with RMSD of 0.781 Å.



(A)



(B)



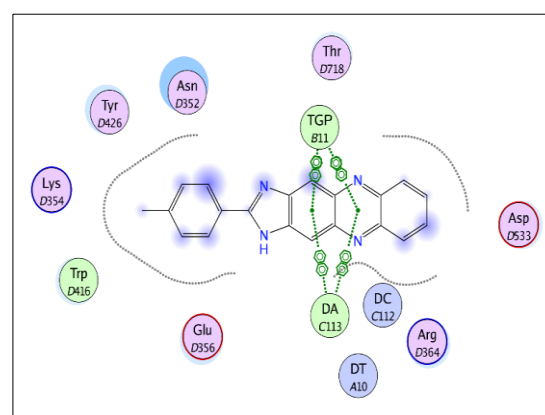
(C)

Fig. 9: (A) 2D interaction diagram showing etoposide docking pose key interactions in topoisomerase II α binding site. (B) 2D diagram and (C) 3D representation showing the superimposition of the co-crystallized (red) and the docking pose (green) of etoposide in topoisomerase II α binding site with RMSD of 1.825 Å.

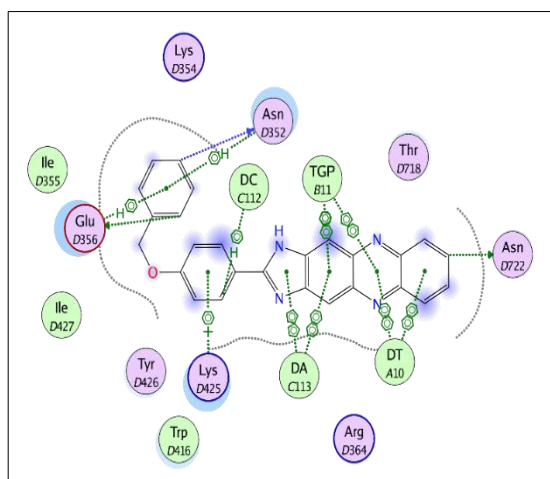
Molecular docking simulations of compounds **4a**, **4e-g** in the target enzymes showed that they adopted common binding modes in each protein like that of the complexed ligands which involve the accommodation of their polycyclic scaffold in the DNA cleavage site stacking between the base pairs interacting through several π - π stacking interactions with the surrounding DNA bases (Fig. 10 and 11). This predicted binding mode could rationalize the biological activity of the target compounds which could be due to their mechanism of action that resembles that of topoisomerase poisons (*vide supra*). The newly synthesized compounds showed promising predicted binding affinity to the target protein with a calculated docking score range of -11.45 to -14.77 kcal/mol and -9.25 to -10.58 kcal/mol in human topoisomerase I and II α , respectively (Table 5).

Table 5. Docking energy scores (*S*) in kcal/mol for the target compounds and the complexed ligands in the topoisomerase I and II α .

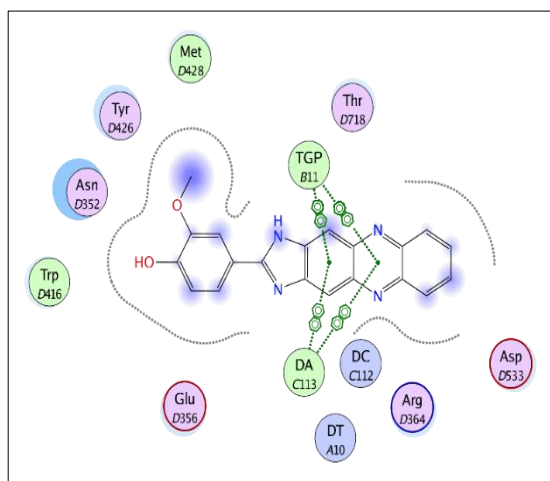
Compound ID	Energy score (<i>S</i>) kcal/mol (PDB ID: 1T8I)	Energy score (<i>S</i>) kcal/mol (PDB ID: 5GWK)
4a	-11.45	-9.25
4e	-14.77	-10.35
4f	-12.74	-10.15
4g	-14.71	-10.58
Camptothecin	-13.24	-----
Etoposide	-----	-15.75



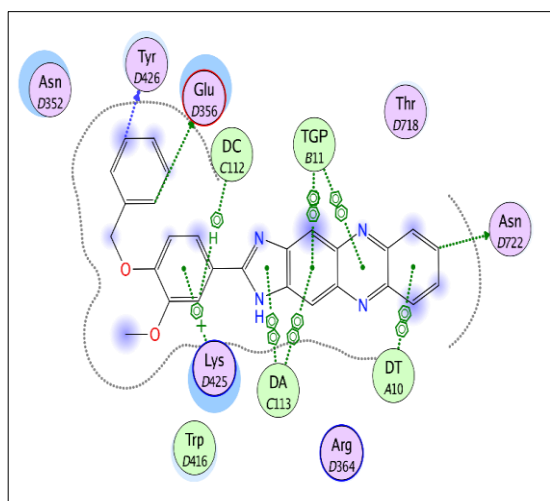
(A)



(B)

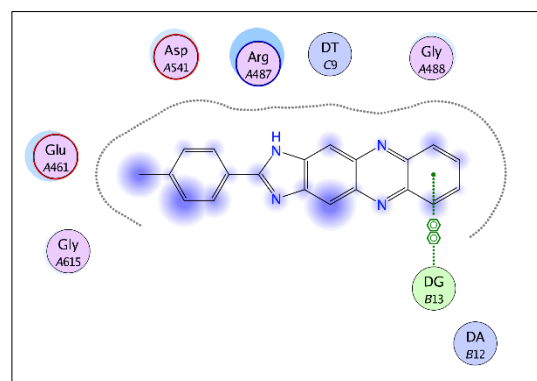


(C)

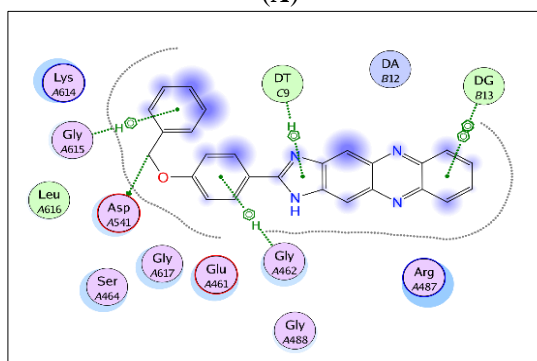


(D)

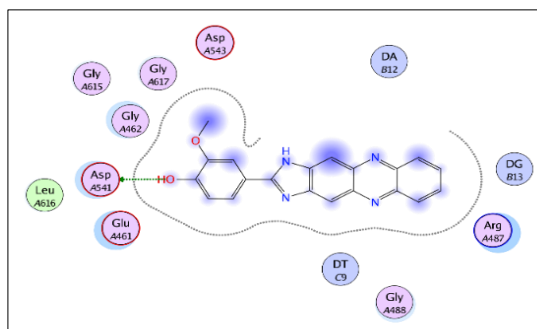
Fig. 10: (A), (B), (C), and (D) 2D interaction diagrams showing compounds **4a**, **4e**, **4f** and **4g** docking pose interactions in topoisomerase I binding site, respectively.



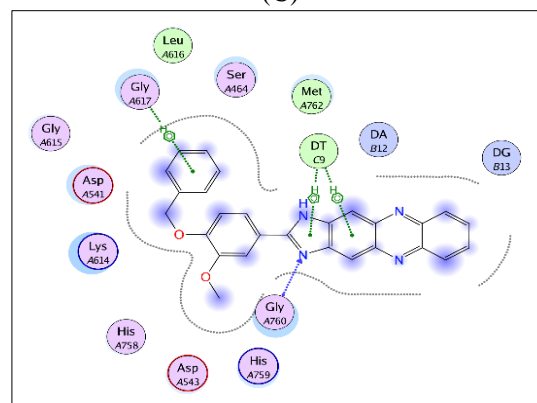
(A)



(B)



(C)



(D)

Fig. 11: (A), (B), (C), and (D) 2D interaction diagrams showing compounds **4a**, **4e**, **4f** and **4g** docking pose interactions in topoisomerase II α binding site, respectively.

3.4. *In silico* prediction of ADME properties of 4a and 4e-g

SwissADME free web tool was utilized for *in silico* prediction of the physicochemical, and the pharmacokinetic properties of the most promising imidazophenazines **4a** and **4e-g** (Table 6) [44]. The obtained results demonstrated that the four promising compounds have molecular weights less than 500, satisfactory topological polar surface area (TPSA), *ilogP* (octanol-water partition coefficient) [45] and water solubility to be well absorbed from GIT. Compounds **4e-g** showed *in silico* inability to penetrate the blood brain barrier which is an advantage to protect the brain from the adverse effects of the chemotherapeutic agents. The predicted bioavailability radar chart displayed that compounds **4a** and **4e-g** have promising physical and chemical properties to be orally bioavailable. Fig. 12 shows the bioavailability radar chart of compounds **4f** and **4g**. The optimum limit for the six properties namely size, polarity, flexibility, lipophilicity, solubility, and the degree of saturation is identified by the zone colored in pink. The submitted compounds are almost present in pink area, only the degree of unsaturation is slightly deviated from the defined border. In addition, the submitted compounds **4a**, **4e-g** fulfill the most acceptable drug-likeness rules including Lipinski's rule, Veber rule, Egan and Muegge's filter. Moreover, they lack Pan Assay Interference compounds (PAINS) fragments in their structures.

Conclusion

A series of 1-(un)substituted-2-(hetero)aryl imidazo[4,5-*b*]phenazines **4a-j** and **6a-d** were synthesized and evaluated for its cytotoxic activity as well as for its topoisomerase inhibitory activity. Based on the structure of the tested candidates, different pattern of cytotoxic activity was observed against the NCI cancer cell lines. The imidazophenazine **4f** turned out to be the most promising candidate against NCI cancer cell lines. It revealed a potent and broad-spectrum anticancer activity with GI% up to 82% against different cancer cell lines. It showed more than 50% growth inhibition against CCRF-CEM, and MOLT-4 cell lines from leukaemia sub-panel, HOP-92 and NCI-H460 cell

lines from non-small cell lung cancer sub-panel, UO-31 cell line from renal cancer sub-panel, and MCF-7 cell line from breast cancer sub-panel.

The most promising imidazophenazines **4a** and **4e-g** were selected to be evaluated for their Topo I and Topo II α inhibitory activities. It was found that compound **4e** is displaying potent Topo I inhibitory activity ($IC_{50} = 29.2 \mu\text{M}$), whereas the imidazophenazines **4f** and **4g** displayed moderate Topo II α inhibitory activities ($IC_{50} = 26.74, 22.72 \mu\text{M}$, respectively) in comparison to camptothecin ($IC_{50} = 25.71 \mu\text{M}$) and etoposide ($IC_{50} = 20.52 \mu\text{M}$) on Topo I and Topo II α , respectively.

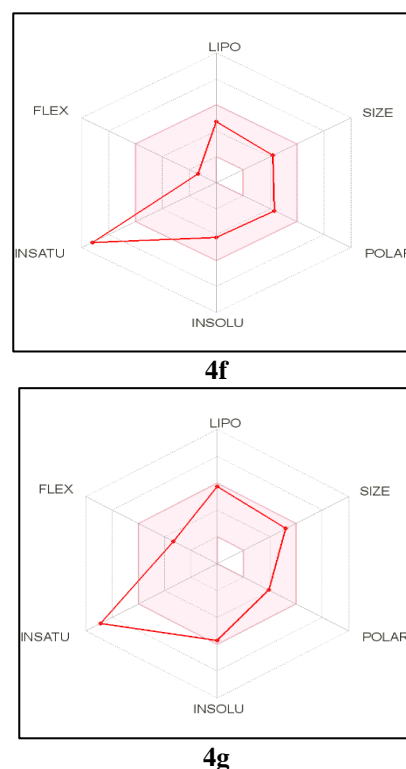


Fig. 12: Bioavailability radar plot of **4f** and **4g**

In summary, the SwissADME results showed that compounds **4f** and **4g** have satisfactory drug likeness profile beside their promising topoisomerase and cancer growth inhibitory activity.

Table 6. Physicochemical and the pharmacokinetic properties of **4a** and **4e-g**

Compound ID	MW	Rotatable bonds	H-bond Acceptor	H-bond Donor	MR	TPSA	Log P	GI absorption	BBB permeant
4a	310.35	1	3	1	97.1	54.46	2.7	High	Yes
4e	402.45	4	4	1	123.11	63.69	3.5	High	No
4f	342.35	2	5	2	100.65	83.92	2.74	High	No
4g	432.47	5	5	1	129.6	72.92	3.58	High	No

Furthermore, compound **4f** caused cell cycle arrest of MCF-7 breast cell line at G2/M phase inducing early and late apoptosis, and necrosis in MCF-7 cells. Molecular docking study on Topo I and Topo II α revealed that the biological activity of the target compounds could be due to their mechanism of action that resembles that of topoisomerase poisons which involves the accommodation of their polycyclic scaffold in the DNA cleavage site stacking between the base pairs interacting through several π - π stacking interactions with the surrounding DNA bases stabilizing the topoisomerase/DNA cleavage complex preventing the re-ligation reaction. SwissADME web tool showed that compounds **4f** and **4g** are not only promising topoisomerase inhibitors and cytotoxic agents, but also with promising physicochemical and pharmacokinetic properties, and drug likeness profile.

Declaration of Interest Statement

The authors declare no conflict of interest to disclose.

Acknowledgments

The authors are grateful for the National Cancer Institute (NCI) [Bethesda, USA] for the anticancer screening of the target compounds.

References

- [1] D. Schottenfeld, J.F. Fraumeni, Cancer epidemiology and prevention, 3rd ed., Oxford University Press, Oxford ; New York, 2006.
- [2] R.L. Siegel, K.D. Miller, H.E. Fuchs, A. Jemal, Cancer Statistics, 2021, *CA Cancer J Clin*, 71, 7-33 (2021).
- [3] S. Singh, D.C. Dhasmana, M. Bisht, P.K. Singh, Pattern of Adverse Drug Reactions to Anticancer Drugs: A Quantitative and Qualitative Analysis, *Indian J Med Paediatr Oncol*, 38, 140-145 (2017).
- [4] B. Mansoori, A. Mohammadi, S. Davudian, S. Shirjang, B. Baradaran, The Different Mechanisms of Cancer Drug Resistance: A Brief Review, *Adv Pharm Bull*, 7, 339-348 (2017).
- [5] S. Salerno, F. Da Settimo, S. Taliani, F. Simorini, C. La Motta, G. Fornaciari, A.M. Marini, Recent advances in the development of dual topoisomerase I and II inhibitors as anticancer drugs, *Curr Med Chem*, 17, 4270-4290 (2010).
- [6] J.L. Delgado, C.M. Hsieh, N.L. Chan, H. Hiasa, Topoisomerases as anticancer targets, *Biochem J*, 475, 373-398 (2018).
- [7] W. Wang, Y.-C. Tse-Dinh, Recent Advances in Use of Topoisomerase Inhibitors in Combination Cancer Therapy, *Current Topics in Medicinal Chemistry*, 19, 730-740.
- [8] J.J. Champoux, DNA topoisomerases: structure, function, and mechanism, *Annu Rev Biochem*, 70, 369-413 (2001).
- [9] J.C. Wang, Cellular roles of DNA topoisomerases: a molecular perspective, *Nat Rev Mol Cell Biol*, 3, 430-440 (2002).
- [10] K.R. Vann, A.A. Oviatt, N. Osheroff, Topoisomerase II Poisons: Converting Essential Enzymes into Molecular Scissors, *Biochemistry*, 60, 1630-1641 (2021).
- [11] Y.R. Wang, S.F. Chen, C.C. Wu, Y.W. Liao, T.S. Lin, K.T. Liu, Y.S. Chen, T.K. Li, T.C. Chien, N.L. Chan, Producing irreversible topoisomerase II-mediated DNA breaks by site-specific Pt(II)-methionine coordination chemistry, *Nucleic Acids Res*, 45, 10861-10871 (2017).
- [12] C.C. Wu, Y.C. Li, Y.R. Wang, T.K. Li, N.L. Chan, On the structural basis and design guidelines for type II topoisomerase-targeting anticancer drugs, *Nucleic Acids Res*, 41, 10630-10640 (2013).
- [13] M. Binaschi, F. Zunino, G. Capranico, Mechanism of action of DNA topoisomerase inhibitors, *Stem Cells*, 13, 369-379 (1995).
- [14] D.A. Burden, P.S. Kingma, S.J. Froelich-Ammon, M.A. Bjornsti, M.W. Patchan, R.B. Thompson, N. Osheroff, Topoisomerase II- ϵ toposide interactions direct the formation of drug-induced enzyme-DNA cleavage complexes, *J Biol Chem*, 271, 29238-29244 (1996).
- [15] V.M. Matias-Barrios, M. Radaeva, Y. Song, Z. Alperstein, A.R. Lee, V. Schmitt, J. Lee, F. Ban, N. Xie, J. Qi, N. Lallous, M.E. Gleave, A. Cherkasov, X. Dong, Discovery of New Catalytic Topoisomerase II Inhibitors for Anticancer Therapeutics, *Front Oncol*, 10, 633142 (2020).
- [16] Y. Pommier, Topoisomerase I inhibitors: camptothecins and beyond, *Nat Rev Cancer*, 6, 789-802 (2006).
- [17] L.F. Liu, S.D. Desai, T.K. Li, Y. Mao, M. Sun, S.P. Sim, Mechanism of action of camptothecin, *Ann N Y Acad Sci*, 922, 1-10 (2000).
- [18] J.L. Nitiss, Targeting DNA topoisomerase II in cancer chemotherapy, *Nat Rev Cancer*, 9, 338-350 (2009).
- [19] W.A. Denny, B.C. Baguley, Dual topoisomerase I/II inhibitors in cancer therapy, *Curr Top Med Chem*, 3, 339-353 (2003).
- [20] G.R. Zimmermann, J. Lehar, C.T. Keith, Multi-target therapeutics: when the whole is greater than the sum of the parts, *Drug Discov Today*, 12, 34-42 (2007).
- [21] C. Viegas-Junior, A. Danuello, V. da Silva Bolzani, E.J. Barreiro, C.A. Fraga, Molecular hybridization: a useful tool in the design of new

- drug prototypes, *Curr Med Chem*, 14, 1829-1852 (2007).
- [22] M. Szumilak, A. Wiktorowska-Owczarek, A. Stanczak, Hybrid Drugs-A Strategy for Overcoming Anticancer Drug Resistance?, *Molecules*, 26, (2021).
- [23] J.B. Laursen, J. Nielsen, Phenazine natural products: biosynthesis, synthetic analogues, and biological activity, *Chem Rev*, 104, 1663-1686 (2004).
- [24] R.W. Huigens, 3rd, B.R. Brummel, S. Tenneti, A.T. Garrison, T. Xiao, Pyrazine and Phenazine Heterocycles: Platforms for Total Synthesis and Drug Discovery, *Molecules*, 27, (2022).
- [25] A. Cimmino, A. Evidente, V. Mathieu, A. Andolfi, F. Lefranc, A. Kornienko, R. Kiss, Phenazines and cancer, *Nat Prod Rep*, 29, 487-501 (2012).
- [26] A.J. Stewart, P. Mistry, W. Dangerfield, D. Bootle, M. Baker, B. Kofler, S. Okiji, B.C. Baguley, W.A. Denny, P.A. Charlton, Antitumor activity of XR5944, a novel and potent topoisomerase poison, *Anticancer Drugs*, 12, 359-367 (2001).
- [27] A.G. Jobson, E. Willmore, M.J. Tilby, P. Mistry, P. Charlton, C.A. Austin, Effect of phenazine compounds XR11576 and XR5944 on DNA topoisomerases, *Cancer Chemother Pharmacol*, 63, 889-901 (2009).
- [28] L.J. Lewis, P. Mistry, P.A. Charlton, H. Thomas, H.M. Coley, Mode of action of the novel phenazine anticancer agents XR11576 and XR5944, *Anticancer Drugs*, 18, 139-148 (2007).
- [29] P. Mistry, A.J. Stewart, W. Dangerfield, M. Baker, C. Liddle, D. Bootle, B. Kofler, D. Laurie, W.A. Denny, B. Baguley, P.A. Charlton, In vitro and in vivo characterization of XR11576, a novel, orally active, dual inhibitor of topoisomerase I and II, *Anticancer Drugs*, 13, 15-28 (2002).
- [30] T. Yamagishi, S. Nakaïke, T. Ikeda, H. Ikeya, S. Otomo, A novel antitumor compound, NC-190, induces topoisomerase II-dependent DNA cleavage and DNA fragmentation, *Cancer Chemother Pharmacol*, 38, 29-34 (1996).
- [31] B.L. Yao, Y.W. Mai, S.B. Chen, H.T. Xie, P.F. Yao, T.M. Ou, J.H. Tan, H.G. Wang, D. Li, S.L. Huang, L.Q. Gu, Z.S. Huang, Design, synthesis and biological evaluation of novel 7-alkylamino substituted benzo[a]phenazin derivatives as dual topoisomerase I/II inhibitors, *Eur J Med Chem*, 92, 540-553 (2015).
- [32] I. Ali, M.N. Lone, H.Y. Aboul-Enein, Imidazoles as potential anticancer agents, *Medchemcomm*, 8, 1742-1773 (2017).
- [33] H.T. Abdel-Mohsen, M.A. Abdullaziz, A.M.E. Kerdawy, F.A.F. Ragab, K.J. Flanagan, A.E.E. Mahmoud, M.M. Ali, H.I.E. Diwani, M.O. Senge, Targeting Receptor Tyrosine Kinase VEGFR-2 in Hepatocellular Cancer: Rational Design, Synthesis and Biological Evaluation of 1,2-Disubstituted Benzimidazoles, *Molecules*, 25, (2020).
- [34] H.T. Abdel-Mohsen, F.A. Ragab, M.M. Ramla, H.I. El Diwani, Novel benzimidazole-pyrimidine conjugates as potent antitumor agents, *Eur J Med Chem*, 45, 2336-2344 (2010).
- [35] M.A. Abdullaziz, H.T. Abdel-Mohsen, A.M. El Kerdawy, F.A.F. Ragab, M.M. Ali, S.M. Abu-Bakr, A.S. Girgis, H.I. El Diwani, Design, synthesis, molecular docking and cytotoxic evaluation of novel 2-furybenzimidazoles as VEGFR-2 inhibitors, *Eur J Med Chem*, 136, 315-329 (2017).
- [36] I. Singh, V. Luxami, K. Paul, Synthesis of naphthalimide-phenanthro[9,10-d]imidazole derivatives: In vitro evaluation, binding interaction with DNA and topoisomerase inhibition, *Bioorg Chem*, 96, 103631 (2020).
- [37] A.T. Baviskar, C. Madaan, R. Preet, P. Mohapatra, V. Jain, A. Agarwal, S.K. Guchhait, C.N. Kundu, U.C. Banerjee, P.V. Bharatam, N-fused imidazoles as novel anticancer agents that inhibit catalytic activity of topoisomerase II α and induce apoptosis in G1/S phase, *J Med Chem*, 54, 5013-5030 (2011).
- [38] J. Sluka, V. Zikan, J. Danek, 2-Phenyl-1H-imidazo(4,5-b)phenazines with anthelmintic effects, *Cesko-Slovenska Farmacie*, 37, 65-70 (1988).
- [39] P. Skehan, R. Storeng, D. Scudiero, A. Monks, J. McMahon, D. Vistica, J.T. Warren, H. Bokesch, S. Kenney, M.R. Boyd, New colorimetric cytotoxicity assay for anticancer-drug screening, *J Natl Cancer Inst*, 82, 1107-1112 (1990).
- [40] P. Peixoto, C. Bailly, M.-H. David-Cordonnier, Topoisomerase I-Mediated DNA Relaxation as a Tool to Study Intercalation of Small Molecules into Supercoiled DNA, in: K.R. Fox (Ed.) *Drug-DNA Interaction Protocols*, Humana Press, Totowa, NJ, 2010, pp. 235-256.
- [41] C. Yu, J. Hu, W. Luyten, D. Sun, T. Jiang, Identification of novel topoisomerase II α inhibitors by virtual screening, molecular docking, and bioassay, *Chemical Biology & Drug Design*, 99, 92-102 (2022).
- [42] I.H. Ali, H.T. Abdel-Mohsen, M.M. Mounier, M.T. Abo-Elfadl, A.M. El Kerdawy, I.A.Y. Ghannam, Design, synthesis and anticancer activity of novel 2-arylbenzimidazole/2-thiopyrimidines and 2-thioquinazolin-4(3H)-ones conjugates as targeted RAF and VEGFR-2 kinases inhibitors, *Bioorg Chem*, 126, 105883 (2022).

-
- [43] B.L. Staker, M.D. Feese, M. Cushman, Y. Pommier, D. Zembower, L. Stewart, A.B. Burgin, Structures of three classes of anticancer agents bound to the human topoisomerase I-DNA covalent complex, *J Med Chem*, 48, 2336-2345 (2005).
- [44] A. Daina, O. Michielin, V. Zoete, SwissADME: a free web tool to evaluate pharmacokinetics, drug-likeness and medicinal chemistry friendliness of small molecules, *Sci Rep*, 7, 42717 (2017).
- [45] A. Daina, O. Michielin, V. Zoete, iLOGP: a simple, robust, and efficient description of n-octanol/water partition coefficient for drug design using the GB/SA approach, *J Chem Inf Model*, 54, 3284-3301 (2014).